A GAIN SCHEDULING APPROACH FOR HYBRID FORCE/VELOCITY CONTROLLED ROBOT CONTOUR TRACKING

G. Ziliani * **F. Jatta** ** **G. Legnani** * **A. Visioli** ***

* *Dipartimento di Ingegneria Meccanica, University of Brescia (Italy), e-mail: {ziliani,legnani}@ing.unibs.it*
** *Istituto di Tecnologie Industriali e Automazione, CNR (Italy), e-mail: f.jatta@itia.cnr.it*
*** *Dipartimento di Elettronica per l'Automazione, University of Brescia, (Italy), e-mail: visioli@ing.unibs.it*

Abstract: This paper deals with the implementation of a hybrid force/velocity controller for the contour tracking of an object of an unknown shape performed by an industrial robot manipulator. In particular we propose the use of a gain scheduling approach in order to cope with the configuration dependent dynamics of the manipulator in constrained motion and therefore in order to allow to obtain satisfactory performances in a very large portion of the robot workspace. Experimental results, obtained with a two degrees-of-freedom SCARA industrial robot manipulator show the effectiveness of the approach.

Keywords: Industrial robots, robot control, force control, robot dynamics, proportional gain.

1. INTRODUCTION

Nowadays industrial settings employ robots in fixed and highly structured environments so that reconfiguration efforts are a clear barrier to face the continuous changes required by the market demand. In order to cope with these limits intelligent robots that are able to autonomously adapt themselves to semi-unstructured tasks are a key issue to cut re-programming costs and to shorten the lead to production time. Automatic tracking of unknown planar contours is an example of an advanced task required by many industrial applications (e.g. grinding, deburring, polishing) where a high degree of autonomy is needed as opposite to standard industrial operations were robots reproduce previously recorded paths with a little amount of feedback from the process under control. Among the all possible force controlled contour tracking strategies, hybrid force/velocity control (Raibert and Craig (1981); Craig (1989)) is one of the most well-known. However, conversely to strategies that employ internal position or velocity loops (Starr (1986); Kazanzides *et al.* (1989); Bossert *et al.* (1996); Yu and Kieffer (1999)), few extensive experimental results appeared in the literature. In particular, experiments that take into account the use of a large portion of the manipulator workspace are often overlooked. Actually, the manipulator dynamic behavior during a constrained motion can be very variable and the stiffness of the joints, the mass of links, the manipulator configuration, the contact direction and the nature of the constraint have to be considered. In this context the tuning of the controller parameters to achieve a satisfactory performance in all the possible planar contour tracking tasks is indeed very difficult.
In this paper, we propose the use of a gain scheduling approach to allow reliable and effective operations in very different working conditions as required by industrial applications.

2. EXPERIMENTAL SETUP

Although the concepts discussed in this paper can be applied in general, in the following we refer to a two-degrees-of-freedom planar industrial SCARA robot, as this is the one adopted in the experiments. The set-up available in the Applied Mechanics Laboratory of the University of Brescia consists of an industrial manipulator manufactured by ICOMATIC (Gussago, Italy) with a standard SCARA architecture where the z-axis has been blocked for our planar tasks. Both links have the same length of 0.33 m. The arm is actuated by two DC motors driven by conventional PWM amplifiers and position measurements are available by means of two incremental encoders with 2000 pulses/rev. resolution. Velocity is estimated through numerical differentiation whose output is then processed by a low-pass 2-order Butterworth filter (100 Hz cut-off frequency and 1.0 damping ratio). An ATI 65/5 Force/Torque sensor capable of measuring forces in a ±65 N range and with a resolution of 0.05N is mounted at the manipulator wrist. The corresponding signals are processed at 7.8 kHz frequency by an ISA DSP based board and collected by the robot controller at 1 kHz. The contact is achieved by means of a proper probe endowed with an 8 mm diameter ball bearing with whose aim is reducing tangential friction forces that may arise from the contact with the piece. The PC-based controller is based on a QNX4 real time operating system and the control algorithms are written in C/C++ language. Acquisition and control are performed at a frequency of 1 kHz.

3. CONTOUR TRACKING

With reference to Figure 1, frame (0) refers to robot base, while task frame (T) has its origin on the robot end-effector, its n-axis is directed along the normal direction of the piece contour and its t-axis along its tangent; ϑ is the angle between axis n and axis x of frame (0). Let $Q = [q_1, q_2]^T$ be the vector of joint positions and $\dot{Q}$, $\ddot{Q}$ its first and second time derivatives respectively. Since a suitable belt transmission keeps the end-effector with constant orientation with respect to the absolute frame, force measurements are directly available in frame (0). Let $F := F_{(0)} = [F_x, F_y]^T$ and $F_{(T)} = [F_t, F_n]^T$ be the vectors of contact force in frame (0) and (T) respectively. They are related to each other by the equation $F = M_{0T}(\vartheta)F_{(T)}$ denoting with M_{ij} the rotation matrix from frame j to frame i. Vector $V_{(T)} = [V_t, V_n]^T$ representing Cartesian velocity in frame (T) can be obtained from the relation

$$V_{(T)} = M_{T0}V_{(0)} = M_{T0}(\vartheta)J(Q)\dot{Q}$$

where $J(Q)$ is the robot Jacobian matrix. The aim of a contour tracking task is to control the normal

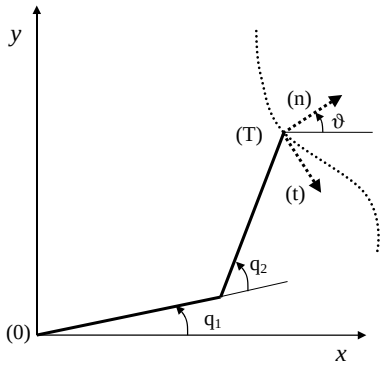

Fig. 1. Sketch of a SCARA robot following a contour.

force and the tangential velocity of the robot probe along n and t directions of task frame (T). These directions can be detected, assuming that the contact friction force on the tangent direction is negligible with respect to the normal contact force (this is achieved by adopting a suitable probe endowed with a ball bearing, as described in Section 2), by on-line estimating the angle ϑ as:

$$\vartheta = \text{atan2}(F_y, F_x) = \arctan\left(\frac{F_y}{F_x}\right) \pm \pi. \quad (1)$$

4. EFFECT OF JOINT ELASTICITIES AND LINK MASSES

It is well known that the dynamics of a robot manipulator can be expressed as:

$$M_q(Q)\ddot{Q} + C(Q,\dot{Q})\dot{Q} + f(\dot{Q}) + G(Q) = \tau - J(Q)^T F$$

where $M_q(Q)$ is the inertia matrix, $C(Q,\dot{Q})$ is the matrix of centrifugal and Coriolis terms, $f = [f_1(\dot{q}_1), f_1(\dot{q}_2)]^T$ is the vector of joint friction forces, $G(Q)$ is the gravity forces term (null in our case), τ is the joint torques vector and F is the already defined vector of forces exerted from the robot to the environment. The elasticity of the speed reducers (and of the transmission shafts), which are typically present in an industrial serial manipulator, may affect the robot behavior in a force control task. Denoting by $\Delta Q = [\Delta q_1, \Delta q_2]^T$ the vector of joint deflections, we assume that, for small deformations, the following linear relation holds:

$$\tau = \chi \Delta Q \quad (2)$$

where $\chi = diag[\chi_1, \chi_2]$ is the 2×2 diagonal matrix containing the joint stiffness parameters for each axis. For a serial robot the following relations express the kinetostatic duality that map joint diplacement/torque to end-effector displacement/force respectively ($\Delta X = [\Delta x, \Delta y]^T$):

$$\Delta X = J(Q)\Delta q, \qquad \tau = J(Q)^T F. \quad (3)$$

Combining equations (3) it follows that:

$$F = K(Q)\Delta X \quad (4)$$

where

$$K(Q) = J(Q)^{-T}\chi J(Q)^{-1} \quad (5)$$

Table 1. Estimated model parameters.

$m_{eq,m}$ [kg]	$m_{eq,M}$ [kg]	m_2 [kg]	k_1 [N/m]	k_2 [N/m]
37	825	2.5	$18 \cdot 10^3$	10^4

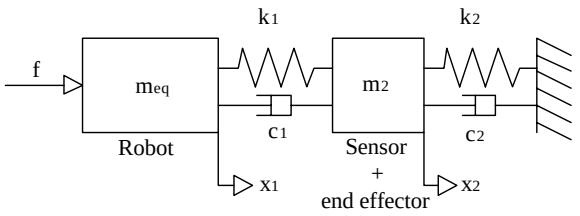

Fig. 2. Model of the manipulator in contact with the environment.

is the configuration dependent stiffness matrix, which maps the displacement of the end effector upon the exertion of the force F due to joint compliance.
The behavior of the manipulator depends on the masses of the links as well. Considering only inertial forces we can write:

$$\tau = M_q \ddot{Q} \tag{6}$$

For a low tracking speed the well known relation $(X = [x, y]^T)$

$$\ddot{X} = \dot{J}(Q)\dot{Q} + J(Q)\ddot{Q}, \tag{7}$$

can be rewritten neglecting the term $\dot{J}(Q)\dot{Q}$ as:

$$\ddot{X} = J(Q)\ddot{Q} \tag{8}$$

and combining it with equation (3) yields:

$$F = M_s(Q)\ddot{X} \tag{9}$$

where $M_s(Q) = J(Q)^{-T} M_q J(Q)^{-1}$ is the configuration dependent inertial matrix, which maps the acceleration of the end effector upon the exertion of the force F due to link masses. An intuitive meaning of the stiffness and inertial behavior of a manipulator expressed by equation (4) and (9) follows from the evaluation of the force required to generate a unit-length displacement and a unitary acceleration respectively at the end effector; calculation of ΔX from equation (4) into $(\Delta X^T)(\Delta X) = 1$ yields:

$$F^T K(Q)^{-T} K(Q)^{-1} F = 1 \tag{10}$$

which represents a stiffness ellipsoid whose principal axis coincide with the eigenvectors of the matrix $K(Q)^{-T}K(Q)^{-1}$ and whose length is equal to the reciprocals of the square roots of the eigenvalues (Tsai (1999)); similarly, an inertial ellipsoid can be obtained for the calculation of $\ddot{X}$ from equation (9) into $\ddot{X}^T\ddot{X} = 1$:

$$\ddot{X}^T M_s(Q)^{-T} M_s(Q)^{-1} \ddot{X} = 1. \tag{11}$$

These equations show that the elastic and inertial behavior of the manipulator is strongly affected by the robot position in the workspace and by the direction of the interaction with the environment.

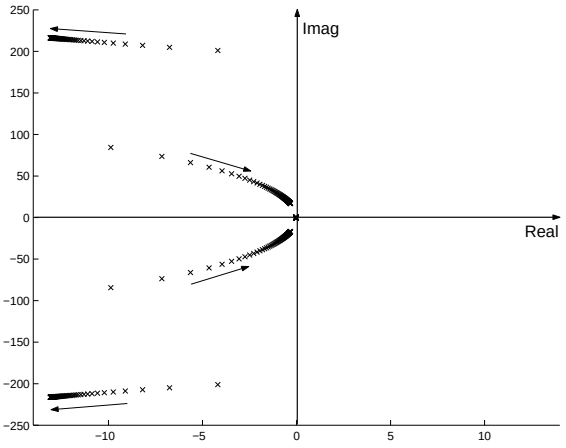

Fig. 3. Poles of the system with a constant K_p at the increasing of the equivalent mass m_{eq}.

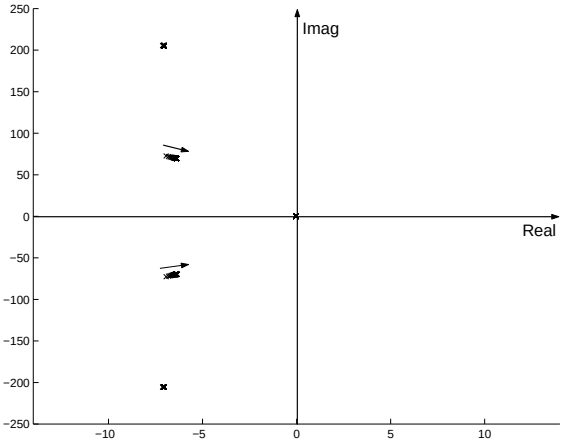

Fig. 4. Poles of the system at the increasing of the equivalent mass m_{eq} with K_p that varies proportionally to m_{eq}.

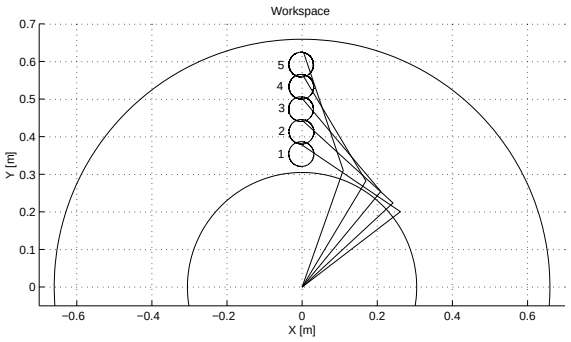

Fig. 5. Different positions of disk in the workspace.

5. CONSTRAINED MANIPULATOR MODEL

To understand qualitatively the influence of the manipulator dynamic parameters on the contour tracking performances, a simplified model of the manipulator in contact with the environment is proposed. The dynamic model parameters have been estimated by means of suitable experiments. In particular, joint stiffnesses were extrapolated by following the method proposed in (Volpe (1990)), while the inertial parameters

were obtained using a least squares procedure (Indri *et al.* (2002)). By considering the resulting high values of $\chi_1 = 35 \cdot 10^3$ Nm/rad and $\chi_2 = 12.6 \cdot 10^3$ Nm/rad, the manipulator arm can be considered as a rigid body, since its equivalent stiffness in any given contact direction, calculated as $n^T K(Q) n$ (where n is the unit vector of contact direction) is much higher than the stiffness (denoted as k_1) of the vertical holder of the end-effector. Thus, the considered model is that shown in Figure 2. The arm is represented as a mass m_{eq} whose position is x_1 and with a force f applied to it. A damping may be present due to friction but the joint friction compensation term in the controller (see Section 6) actually keeps its influence low and so this term can be neglected.

The value of the equivalent mass for a given arm configuration and direction of contact can be calculated as:

$$m_{eq} = n^T M_s(Q) n = n^T J(Q)^{-T} M_q J(Q)^{-1} n \tag{12}$$

Since the force sensor is very stiff and rigidly connected to the end effector, we can describe them as a single mass m_2 connected to the arm by a spring k_1 and a damping c_1. The sensor is in contact with the environment through a plastic probe whose stiffness and damping are denoted respectively as k_2 and c_2. The environment is supposed to be perfectly stiff.

The values of the dynamic parameters of the considered model are reported in Table 1. Note that for m_{eq} we reported the minimum and maximum values (denoted as $m_{eq,m}$ and $m_{eq,M}$ respectively) determined by considering a large part of the workspace. Indeed, m_{eq} tends to infinite at the limit of the robot workspace, where the two links are aligned (i.e. a singular configuration occurs) and therefore the limit has been reduced of 30 mm. Regarding the values of the damping terms c_1 and c_2 they are very difficult to estimate and the reasonable values of $c_1 = 50$ and $c_2 = 20$, have been selected (Volpe (1990)). In any case, changing these values do not affect significantly the results.

Let a PI force control be applied to this system:

$$F(s) = K_p \left(1 + \frac{1}{T_i s}\right) (F_s(s) - F_d(s)) \tag{13}$$

where $F(s)$, $F_s(s)$ and $F_d(s)$ are respectively the Laplace transforms of f, $f_s = k_2 x_2 + c_2 \dot{x}_2$ which is the measured contact force, and f_d which is the desired force set point. As an example, Figure 3 illustrates how the position of the poles of the resulting closed-loop transfer function typically changes when constant values of the proportional gain ($K_p = 14$ in this case) and of the integral time constant ($T_i = 30$) are applied, whilst the value of m_{eq} increases within its range. Conversely, maintaining the same value of T_i, if K_p varies proportionally to m_{eq} (e.g. $K_p = m_{eq}/3.5$) then we obtain the result plotted in Figure 4.

Although just a qualitative analysis can be been performed using the simplified model of Figure 2 (the actual system is obviously time-variant and nonlinear), this suggests the use of a gain scheduling approach to cope with the configuration dependent dynamics of the manipulator during a contour tracking task.

6. HYBRID FORCE/VELOCITY CONTROL

The following hybrid force/velocity control law has been initially considered:

$$\tau = J^T(Q) M_{0T} (U_{(T)} + K_R R) + \hat{f} \tag{14}$$

where $R = [V_{t,d}, F_{n,d}]^T$ is the feedforward vector based on the force and the velocity references, $K_R = diag[k_{V,ff}, k_{F,ff}]$ the corresponding diagonal matrix of gains, $\hat{f} = [\hat{f}_1(\dot{q}_1), \hat{f}_1(\dot{q}_2)]^T$ is an available estimate of the joint friction torques (Jatta *et al.* (2002)) and

$$U_{(T)} = [u_{PID,V}, \quad u_{PI,F} + K_{v,fb}(V_{n,d}(t) - V_n(t))]^T$$

where $u_{PID,V}$ is the tangential velocity PID output, $u_{PI,F}$ is the normal force PI output, $V_{n,d}(t) = 0$, $V_n(t)$ is the velocity of the end-effector in the normal direction and $K_{v,fb}$ is a proportional gain. Note that the use of a normal force derivative term has been substituted with a normal force velocity feedback loop (Craig (1989)).

An extensive experimental campaign has been made to find out the dependence of the contour tracking performances on the configuration and on the contact force direction. In particular, a metallic disk with a diameter of 60 mm, placed in different positions along the y-axis with increasing distance from the origin, has been tracked by employing the control law (14) with a standard force PI controller. The normal force setpoint was 20 N, while the tangential velocity setpoint was 5 mm/s. The relatively small diameter of the piece, compared to the manipulator size, allows the study of the effect of the force direction variation only, because during the path following the manipulator configuration does not change significantly while the contact force makes a complete revolution. The positions of the disk in the robot workspace and the corresponding robot configurations are reported in Figure 5. Figure 6 shows in the left column the inertial ellipsoids calculated from equation (11) for the disk in different positions and in the central column the normal force error collected during the tracking of the disk (in the clockwise direction, starting from the point indicated by a small arrow). Note that only the last three disks have been considered since the results for the first two disks are very similar to the third one. The normalized force error has been plotted on the path reconstructed using the forward kinematics. Comparing these figures it is possible to recognize that, in general, the zones that present low equivalent mass in the contact force direction match with the zones where large and rapid force error oscillations occur. This can be explained considering that the proportional gain has been tuned

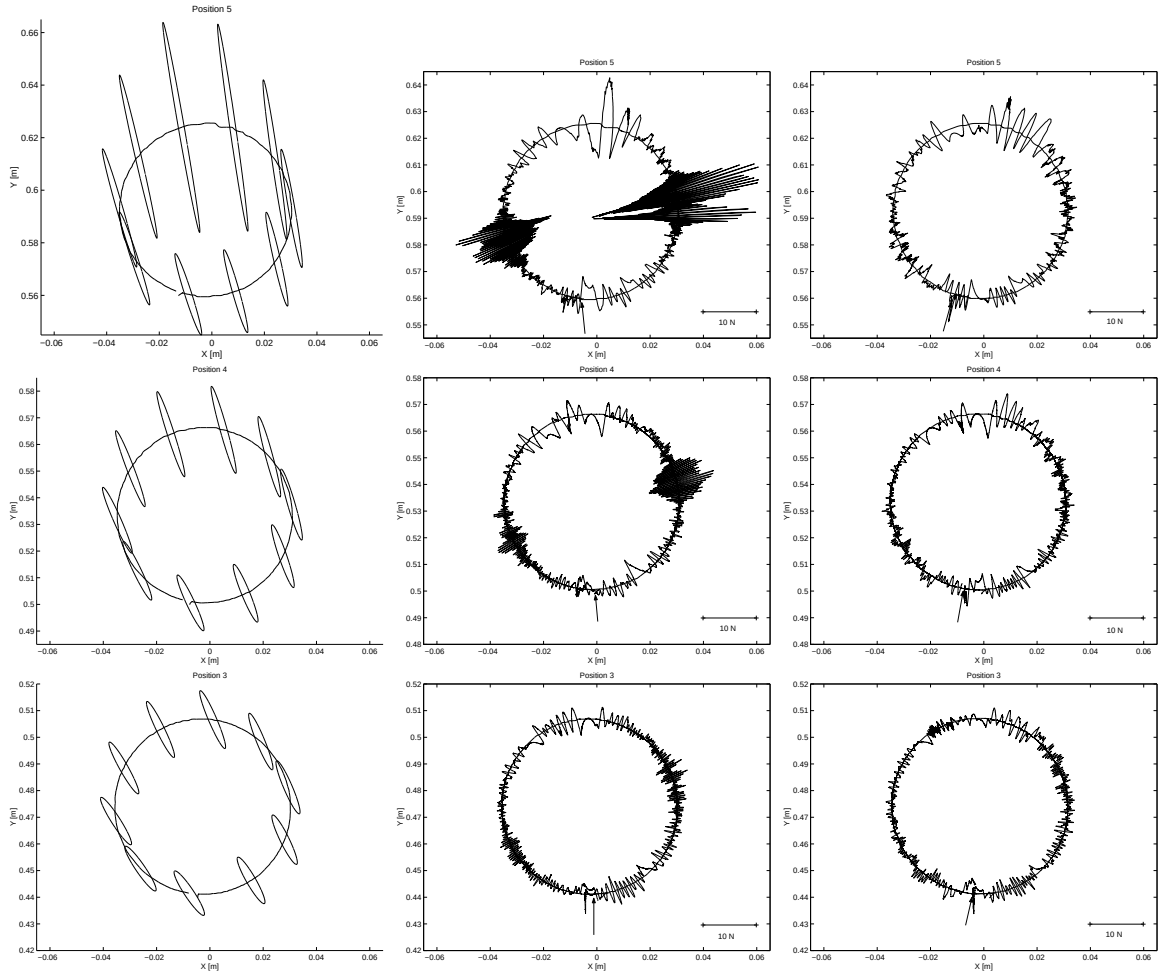

Fig. 6. Inertial ellipsoids (left column) and normal force errors obtained with a standard PI controller (central column) and with the gain scheduling approach (right column) for different disk positions.

for a medium value of the equivalent mass and as the value of m_{eq} decrease the (corresponding) too high value of K_p tends to reduce the damping of the system. Actually, as the robot end-effector get closer to the limit of the workspace, i.e. for positions 4 and 5 of the disk, indeed the force error amplitude in some configurations reaches values that might yield to the loss of the contact. Detuning the (constant) proportional gain brings a reduction of oscillations but makes the robot to detach where the equivalent mass is higher.

The previous results motivates the use of a gain scheduling approach in the force PI controller, i.e. the adoption of a time varying proportional gain (the integral time constant is maintained constant). The value of the proportional gain K_p is allowed to vary in a given interval whose endpoint values $K_{p,min} = 0.005$ and $K_{p,max} = 0.13$ have been chosen with an extensive trial-and-error procedure in such a way that they are appropriate (constant) values for low and high equivalent mass respectively (note that the original K_p was equal to 0.03).

Thus, the value of the proportional gain K_p of the force PI controller depends proportionally on the equivalent mass m_{eq} in the contact force direction, according to the expression

$$K_p = K_{p,min} + (m_{eq} - m_{eq,m}) \frac{K_{p,max} - K_{p,min}}{m_{eq,M} - m_{eq,m}}.$$

7. EXPERIMENTAL RESULTS

The gain scheduling approach has been tested by repeating with the modified controller the same experiments of Section 6. The normalized force errors have been plotted on the path reconstructed with forward kinematics in Figure 6 (right column). A clear improvement in the performances obtained by employing a gain scheduling approach appears. Actually, comparing the results, it can be seen that high amplitude force oscillations disappear in the zones with low equivalent mass and no significant variations in the performances are noticed in the other zones.

To test further the performances of the new controller a wooden piece of a very complex shape has been tracked. The shape covers a great part of the manipulator workspace and presents convex and concave curves (see Figure 7 where the stiffness ellipsoids are plotted along the path). The tangential velocity setpoint is 20 mm/s and the contact force setpoint is 20 N. The piece was tracked in the counterclockwise direction. The

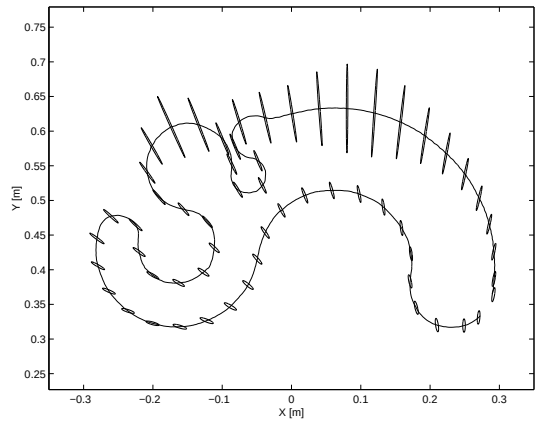

Fig. 7. Inertial ellipsoids for the piece with a complex shape.

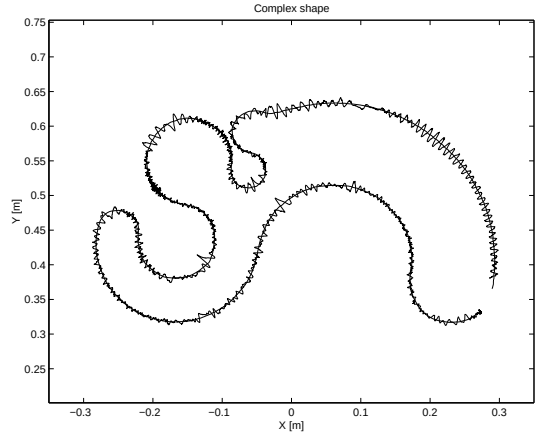

Fig. 8. Normalized force errors during the contour tracking of the complex shape.

contact force error plotted on the reconstructed path is plotted in Figure 8. It has to be stressed that without the use of a gain scheduling it was not possible to accomplish the task due the numerous losses of contact. The normalized value of the proportional gain of the force PI controller (scheduled) proportional gain depending of the contact point is plotted in Figure 9. Summarizing, it results that, despite high performances are achieved with the original controller when the (unknown) piece to track is situated in a large portion of the workspace, this portion is significantly widen by employing the devised gain scheduling approach. A video of the experiment is available at `robotics.ing.unibs.it/gs.htm`.

8. CONCLUSIONS

In this paper we have shown that the use of a gain scheduling approach can significantly improve the performances achieved by a hybrid force/velocity controller in the contour tracking task of an unknown piece performed by an industrial robot manipulator. In particular, the adoption of a time-varying proportional gain of the normal force PI controller allows to enlarge the portion of the workspace area that can be employed by the robot and therefore to obtain similar performances for different tasks which is a fundamental prerequisite for applications in the industrial context.

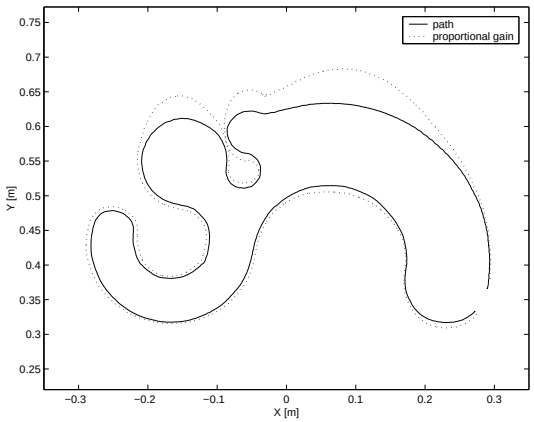

Fig. 9. Normalized values of the (scheduled) proportional gain plotted on reconstructed path.

REFERENCES

Bossert, D., U. Ly and J. Vagners (1996). Experimental evaluation of a hybrid position and force surface following algorithm for unknown surfaces. In: *Proc. IEEE Int. Conf. on Robotics and Automation*. pp. 2252–2257.

Craig, J. J. (1989). *Introduction to Robotics: Mechanics and Control, 2nd edition*. Addison-Wesley. New York, USA.

Indri, M., G. Calafiore, G. Legnani, F. Jatta and A. Visioli (2002). Optimized dynamic calibration of a SCARA robot. In: *Preprints XV IFAC World Congress on Aut. Cont.*. Barcelona, E.

Jatta, F., R. Adamini, A. Visioli and G. Legnani (2002). Hybrid force/velocity robot contour tracking: an experimental analysis of friction compensation strategies. In: *Proc. IEEE Int. Conf. on Robotics and Automation*. pp. 1723–1728.

Kazanzides, P., N. S. Bradley and W. A. Wolowich (1989). Dual-drive force/velocity control; implementation and experimental results. In: *Proc. IEEE Int. Conf. on Robotics and Automation*. pp. 92–97.

Raibert, M. H. and J. J. Craig (1981). Hybrid position/force control of manipulators. *ASME Journal of Dynamic Systems, Measurements, and Control* **102**, 126–133.

Starr, P. (1986). Edge-following with a puma 560 manipulator using val-ii. In: *Proc. IEEE Int. Conf. on Robotics and Automation*. pp. 379–383.

Tsai, L.W. (1999). *Robot Analysis - The Mechanics of Serial and Parallel Manipulators*. John Wiley & Sons.

Volpe, R. (1990). Real and artificial forces in the control of manipulators: Theory and experiments. PhD thesis, Carnegie Mellon University.

Yu, K. and J. Kieffer (1999). Robotic force/velocity control for following unknown contours of granular materials. *Control Engineering Practice* **7**, 1249–1256.